



Combined Diagnosis of Partial Discharge Based on the Multi-dimensional Characteristic Parameters

Weiqliang Qi^a, Yuan Gui^a, Dapeng Duan^a, Songlin Zhou^a, Jianpeng Dong^b

^aBeijing Electric Power Research Institute, Fengtai, Beijing, China

^bSchool of Electrical Engineering, Wuhan University, Wuhan, China

Abstract.

This paper presents a comprehensive multi-parameter diagnosis method based on multiple partial discharge signals include high-frequency current, ultrasound, ultrahigh frequency (UHF) etc. First, acquire the high-frequency current, ultrasound, UHF partial discharge data under various types of defects, and extract the characteristic values, including nine basic characteristic parameters, eight phase characteristic parameters and the like. Diagnose signals respectively, with the method based on information fusion and semi-supervised learning for high-frequency current PD data, the method based on adaptive mutation parameters of particle entropy for ultrasonic signals, the method based on IIA-ART2A neural network for UHF signals. Then integrate the diagnostic results, which is the probability of fault of various defects and matrix, of different PD diagnosis signals, and analysis with the multiple classifier based on multi-parameter fuzzy integral to get the final diagnosis.

1. Introduction

In the electric field, only part of the power equipment insulation portion generates a discharge, but the phenomenon that a fixed discharge channel is not formed in the discharge area called partial discharge (hereinafter referred to as PD). PD can effectively reflect the presence of insulation defects inside the power equipment. At the same time, the development of PD will accelerate the insulation deterioration of the internal power equipment, leading to internal electrical equipment insulation fault occurs, resulting in equipment fault and reduce the reliability of power supply. Therefore, it is necessary to monitor the existence of partial discharge in electrical equipment, as well as the type of discharge, early detection of equipment insulation defects, to deal with it in time, and to avoid the failure of electrical equipment, reduce the serious economic losses caused by power equipment insulation fault [1–3].

At present, at home and abroad the available PD charging detection methods include ultrasonic method, UHF method and high-frequency current method, these types of detection methods are non-invasive ways to detect, a single partial discharge detection method face the problems such as large limitations on detecting range, high probability of partial discharge misjudgment and other issues [4–6]. The combined diagnosis of partial discharge based on the multi-dimensional characteristic parameters brought by this paper use joint diagnostic method based on multi-parameter fuzzy integral to process the collected signals. A large number of experimental data show that the method for partial discharge signal has high diagnostic accuracy and is able to judge the internal insulation of electrical equipment better.

2010 *Mathematics Subject Classification.* 28E10.

Keywords. Multi-parameter fuzzy integral; Partial discharge; Combined diagnosis; Characteristic parameters.

Received: 9 September 2017; 1 November 2017

Communicated by Hari M. Srivastava

Email addresses: weiqiangqi@qq.com (Weiqliang Qi)

2. Single partial discharge diagnosis algorithm

2.1. High-frequency current PD data's diagnostic method based on information fusion and semi-supervised learning

In this paper, for the diagnosis of high-frequency current PD data, we take the method based on information fusion and semi-supervised learning, which is shown in the flow chart in Figure 1.

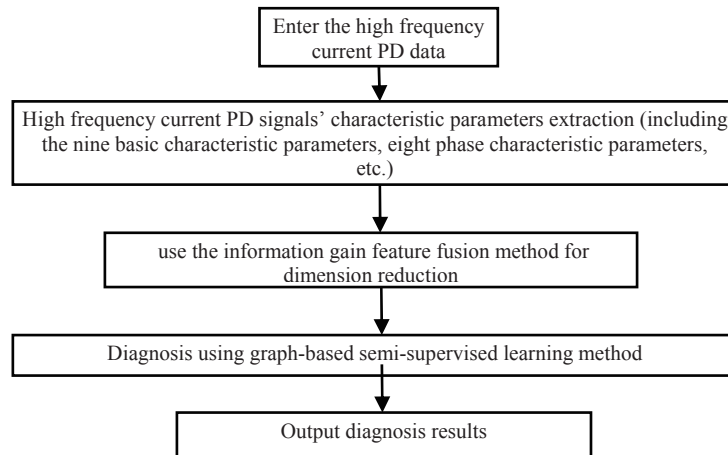


Figure 1: The flow chart of diagnosis method based on information fusion and semi-supervised learning for high-frequency current PD data

The specific implementation steps of the algorithm can be described as follows:

Given a data collection $X = \{x_1, x_2, \dots, x_l, x_{l+1}, \dots, x_n\}$ and a tag collection $C = \{1, 2, \dots, c\}$, in which the first l ones $x_i (i \leq l)$ are already labeled samples, labeled as $y_i \in \{1, 2, \dots, c\}$, and the last u ones $x_i (l + 1 < i \leq n)$ are unlabeled samples. The targets are the labels of predicted unlabeled samples. Define a $n \times c$ matrix $F = [F_1^T, \dots, F_n^T]^T$. $F_i (i \in 1 \dots n)$ is the energy vector of x_i and x_i is tagged as $y_i = \arg \max_{j < c} F_{ij}$. Define the initial $n \times c$ matrix Y ,

$$Y_{ij} = \begin{cases} 1 & x_i, y_i = j \\ 0 & \end{cases} \quad (1)$$

Steps of iterative solver are as follows:

1) Construct undirected weighted graph $G = (X, E)$, X is a collection of samples and E is a set of Edges of figure G ;

2) Construct similar matrix K ;

3) calculate the matrix L with $L = D^{-1/2}KD^{-1/2}$, D is the diagonal matrix and the diagonal elements

$$D_{ii} = \sum_{k=1}^{l+u} K_{ik} \quad (2)$$

4) iterative solve with $F(t + 1) = \alpha LF(t) + (1 - \alpha)Y$ until convergence, where the parameter $\alpha (0 < \alpha < 1)$ representing the category information obtained from a neighboring node, t for the current iteration steps. Initial iteration take $F(0) = Y$;

5) When $F_{ij} > F_{ik} (k \neq j)$, mark each x_i as $y_i = j$.

In the four types of discharge model, the recognition result of semi-supervised learning method is shown in Table 4. We can see that the accuracy rate of spike discharge is 77%, particulate discharge is 83%, suspended discharge is 83% and air discharge is 83%.

Table 1: The recognition result of semi-supervised learning method

Defect type	Spike	Particulate	Suspended	Air
Spike	770	107	51	72
Particulate	23	830	36	111
Suspended	34	65	860	41
Air	62	143	55	740

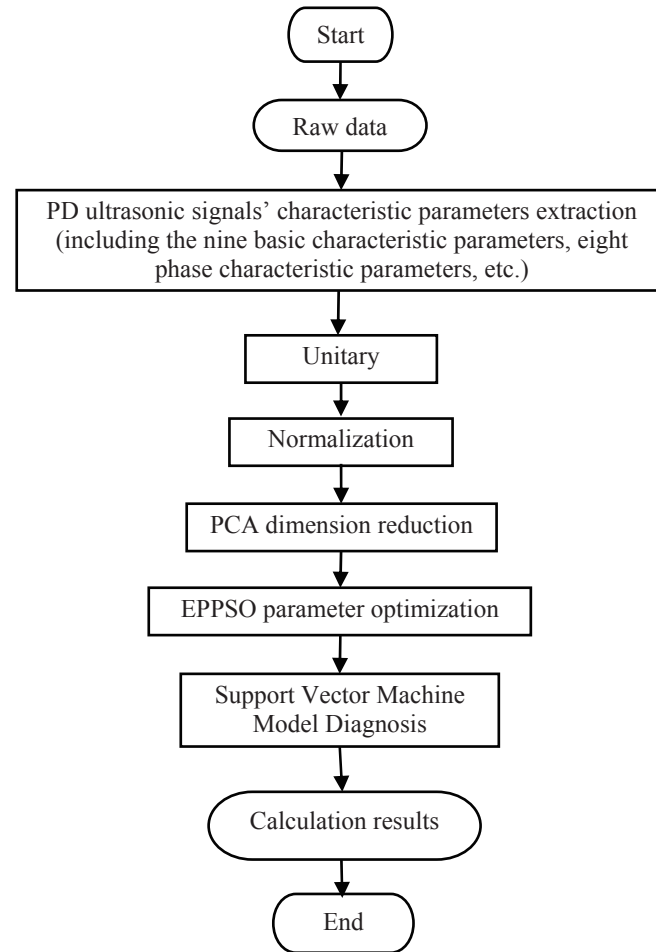


Figure 2: The flow chart of diagnosis method based on adaptive mutation parameters of Particle entropy for ultrasonic signals

2.2. Ultrasonic signals diagnostic method based on adaptive mutation parameters of particle entropy

In this paper, the parameters are optimized with a method based on particle entropy parameter adaptive mutation, and then used for PD ultrasound data' diagnosis. The flow chart is shown in Figure2.

Process of parameters' adaptive mutation algorithm based on particle entropy (referred to as EPPSO, PSO based on Swarm Entropy) proposed in this paper are as follows:

- (1) Randomly determine the initial position and velocity of each particle in the data field, and set E_0 as the stable threshold value of particle entropy;
- (2) Set the particles' pbest to the current optimal position, and set p_{gd} as the global optimal position of initial population;
- (3) Update the position and velocity of the particles;

- (4) If the particle fitness is better than the fitness of p_{gd} , update p_{gd} with the current position;
- (5) Calculate the collection of particle entropy and determine whether the entropy of each particle is less than the predetermined threshold value E_0 , perform (6) when it is true, otherwise skip;
- (6) Vary w to w_0 , calculate the variation value of p_{gd} , then continue to update the iteration;
- (7) Determine whether the convergence criteria of algorithm (fitness variance is less than the set value) are met, if true, implement (8); otherwise, continue iterating;
- (8) Output p_{gd} and end the algorithm.

2.3. UHF signal diagnostic method based on neural network IIA-ART2A

In this paper, parameters of ART2 neural network are optimized with a method based on immune algorithm with the improved variation of natural cycle, then used for the UHF PD data diagnostic [8–12]. The flowchart is shown in Figure 3.

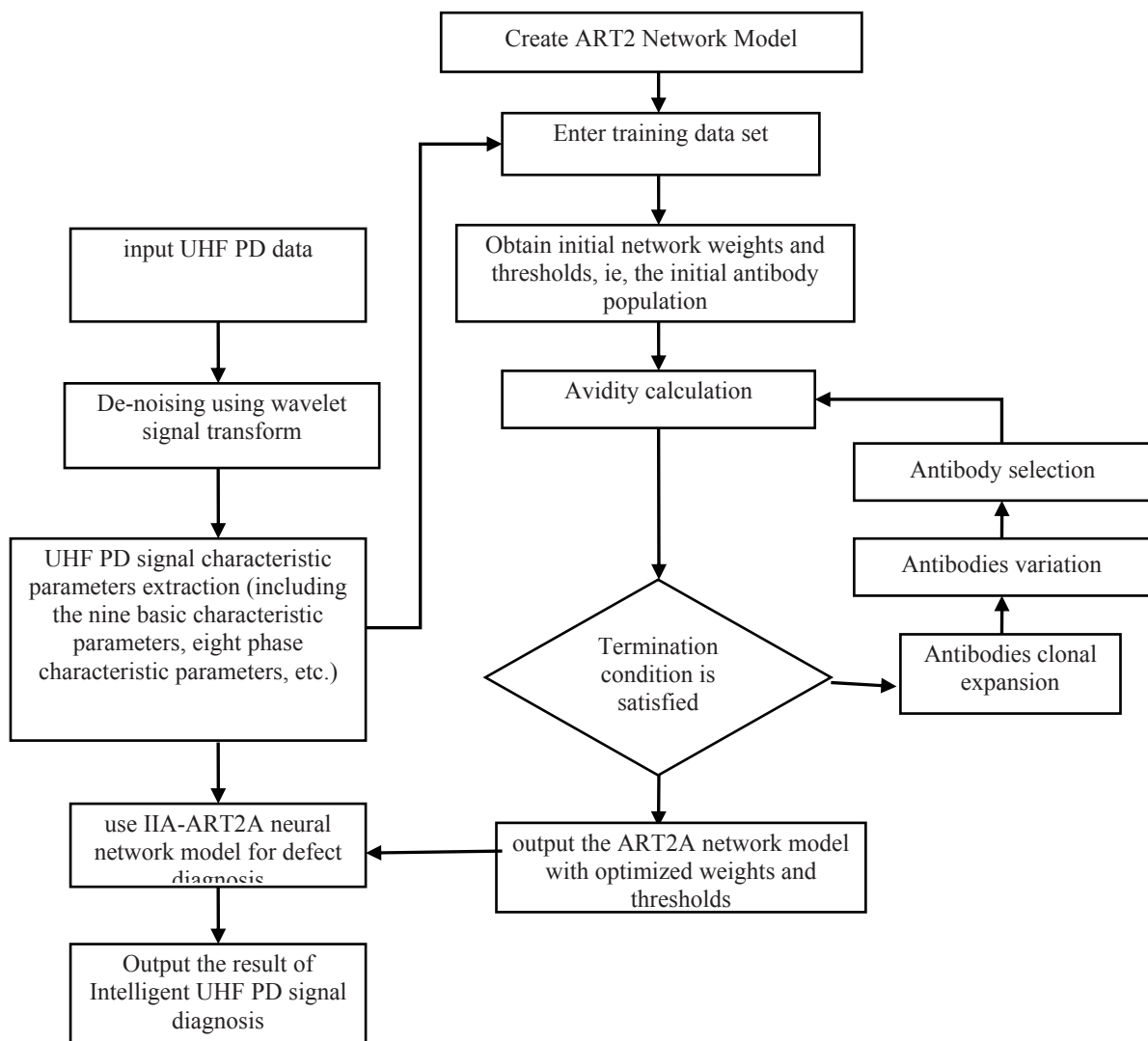


Figure 3: The flowchart of UHF signal diagnostic method based on neural network IIA-ART2A

IIA-ART2A network is unsupervised learning, so it doesn't require the number of training sample, but the training sample to be able to reflect the substance of the mapping problem. Just select the correct

input vector, only a few samples you can get high recognition accuracy. And because ART2A has the characteristics of studying while running, for a new input sample, it can both train learning and test its recognition accuracy.

From the results of the training we are basically able to see the success rate of the network’s recognition is very high. 1000 new sample data was selected in each type of defect, characteristic parameters were extracted and pattern recognition with IIA-ART2A neural networks. Its recognition results are shown in Table, where the fractal dimension numerical lists only the 4th node of 4 floor wavelet packet decomposition, and matching nodes 1-4 represent spike, particulate, suspended and air respectively. We can see that the correct recognition rate of spike discharge is 91%, particulate discharge is 85%, suspended discharge is 84% and air discharge is 77%.

Table 2: the recognition result of IIA-ART2A network

No.	fractal dimension	damp coefficient	similarity	matching node
0	0.072	0.01	0.9912	1
1	0.183	0.001	1	2
2	0.183	0.001	1	2
3	0.071	0.01	0.9912	1
.....

3. Multiple classifier’s fusion analysis based on multi-parameter fuzzy integral

In this paper, we take a multiple classifier fusion method based on multi-parameter fuzzy integral, to integrate the final diagnosis matrix (the probability of failure of various defects) of different PD diagnosis signals (high-frequency current, ultrasound and UHF) and calculate the final diagnosis result [13–17]. The flowchart is shown in Figure 4.

Fault diagnosis is essentially a decision-making process of classification, improving the classification accuracy by increasing complexity of individual classifier is often unsatisfactory, while it is a wise choice to improve the overall classification accuracy by fusing various classifiers with relatively simple structure. Thus combining a plurality of different classifiers to obtain high accuracy is an important research topic today. There is interaction between the classifier, rather than independent. Fuzzy integral is non-linear integral based on fuzzy measurement, and fuzzy measurement is a non-negative non-additive set function, while the non-additive characteristic of fuzzy measurement can precisely describe interactions between classifiers. Therefore, exploring fusion technology of multiple classifiers based on fuzzy integral is the content of this article.

Let $C = \{C_1, C_2, \dots, C_n\}$ be a collection of n target-categories, $X = \{x_1, x_2, \dots, x_m\}$ is a collection of m classifiers. Z_k is the k th identified object. After sample Z_k is identified by each classifier, we can get a matrix referred to as $DP(Z_k)$, which is the cross-section in decision-making model.

$$DP(Z_k) = \begin{bmatrix} h_{11}^k & h_{12}^k & \dots & h_{1n}^k \\ \dots & \dots & \dots & \dots \\ h_{i1}^k & h_{i2}^k & \dots & h_{in}^k \\ \dots & \dots & \dots & \dots \\ h_{m1}^k & h_{m2}^k & \dots & h_{mn}^k \end{bmatrix} \tag{3}$$

And each row vector $h_i = (h_{i1}^k, h_{i2}^k, \dots, h_{in}^k), (i = 1, 2, \dots, m)$ is the recognition results of a classifier x_i on the sample Z_k in various categories, we call it output vector of classifier x_i . Each column vector $h_j = (h_{1j}^k, h_{2j}^k, \dots, h_{mj}^k), (j = 1, 2, \dots, n)$ represents recognition results of each classifier on the sample Z_k in category C_j , we call it fusion vectors of. When the sample is fixed, h_j can be thought of as a function $h_j : X \rightarrow [0, 1]$ (if the output of the classifier is not in the interval $[0, 1]$, it can be normalized to meet the conditions), which maps the classifier x_i to the corresponding components h_{ij} of fusion vector C_j . Each

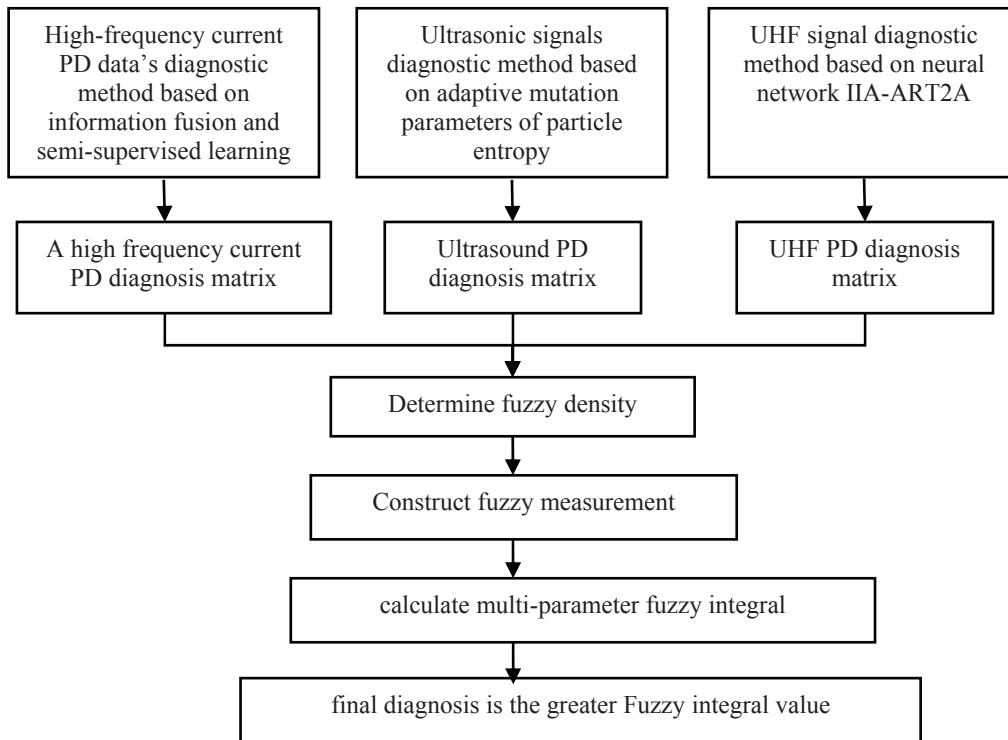


Figure 4: The flowchart of combined diagnosis method based on multi-parameter fuzzy integral.

intersection h_{ij}^k of the output vector x_i and the fusion vector C_j represents the degree of determination on that the class classification x_i assigned sample Z_k to category C_j , also known as the objective estimate of the determination that Z_k belongs to C_j of the classifier x_i . When $h_{ij}^k = 1$, the classifier x_i determines Z_k belongs to the category C_j ; on the contrary, when $h_{ij}^k = 0$, x_i confirms that Z_k does not belongs to category C_j .

Let g is the multi-parameter fuzzy measurement of the defined power set $P(X)$ of X , fuzzy measurement on a single set of points (the fuzzy density) $g^j = g(\{x_i\})$, ($i = 1, 2, \dots, m$) indicates the credibility of the decisions made by classification x_i . $\forall A \in P(X)$, $g(A)$ represents degree of reliability of local decision made by a subset A of X . Fuzzy integral fuse the objective evaluation of the determination that Z_k belongs to C_j (fusion vectors of C_j) and the degree of reliability of classifiers credibility, the integral value is the total objective evaluation of the system that the sample belongs to category C_j . Thus, the system has integrated value for each category, taking the corresponding category of maximum integrated value as the system's determined category of sample Z_k .

Therefore, the basic steps of fusion with fuzzy integral can be summarized as follows:

- ① Determine fuzzy density;
- ② Construct fuzzy measurements. Parameters are determined through the Fuzzy density, then fuzzy measurements are also determined;
- ③ Calculate fuzzy integral. The integrated extent of determination of the fused object to be identified belonging to each category;
- ④ Size comparison of the integral value, to determine the category of the object to be identified.

In order to facilitate the integration of fuzzy arithmetic, we must first set the output the probability of failure, provided w_i ($i = 1, 2, \dots, m$) the corresponding characteristic parameters' values of sample data and

the m -th fault, the occurrence probability of the i -th fault is defined as:

$$\eta_i = \frac{w_i}{w_i + w_k}, w_k = \min_{k=1,2,\dots,m, k \neq i} (w_k) \tag{4}$$

And, $0 < \eta_i \leq 1$, η_i has a clear sense, it reflects the difference between the binding energy of sample and the i -th fault and the binding energy of sample and the fault second to the i -th. When the two values are equal $\eta_i = 0.5$, critical state $\eta_i > 0.5$, it can be classified as i type, and the greater the value of η_i the stronger the deterministic of classification.

PD fault Data of four state including spikes on the surface of high-voltage conductor, free metal particulates, suspended electrode and a solid insulating gap, take 1000 samples from each state, within which training samples change depending on the conditions, 500 test samples, and construct classifiers of three categories:

① Classifier 1, take 1000 training samples, construct M1 classifier in accordance with the proposed high-frequency current PD data’s diagnostic method based on information fusion and semi-supervised learning;

② Category 2, take 1000 training samples, construct M2 classifier in accordance with the proposed ultrasonic signals diagnostic method based on adaptive mutation parameters of particle entropy ;

③ Category 3, take 1000 training samples, construct M3 classifier in accordance with the proposed UHF signal diagnostic method based on neural network IIA-ART2A.

Accuracy rates obtained when identifying four types of samples are shown in Table 6.

Table 3: accuracy of the classifiers

Defect model	Total number of testing samples	Total number of training samples	M1	M2	M3
A spike	1000	500	0.77	0.81	0.91
B particulate	1000	500	0.83	0.77	0.85
C suspended	1000	500	0.86	0.76	0.84
D air	1000	500	0.74	0.84	0.77

Fuzzy density is defined based on the accuracy of the method, then the fuzzy density matrix is ??obtained:

$$DP = \begin{bmatrix} 0.2592 & 0.2577 & 0.2737 \\ 0.2645 & 0.2338 & 0.2465 \\ 0.2419 & 0.2628 & 0.2593 \\ 0.2581 & 0.2255 & 0.2367 \end{bmatrix} \tag{5}$$

Take a test sample as an example, the sample is identified by the M1, M2, M3 classifiers, calculate the probability of its belonging to A, B, C, D categories according to the formula (6.9), then directly classified, it is divided into class D by M1 and M3, into A category by M2.

Table 4: the conversion of probability on sample characteristics among different classifiers

Defect model	M1	M2	M3
A spike	0.2514	0.5423	0.3525
B particulate	0.1375	0.2585	0.2352
C suspended	0.4686	0.3242	0.1554
D air	0.7445	0.5186	0.6673

Table 8 shows the results of fuzzy measure and fuzzy integral, within which $h(x)$ is measurable function, the results of the descending corresponding item in Table 8, $g(\bullet)$ is the fuzzy measurement calculated according to the rank of fuzzy density and measurable function $h(x)$, S_v express the multi-parameter fuzzy

integral value of $h(x)$ and $g(\bullet)$, wherein the fuzzy density is calculated from the classification accuracy. Make judgments based on the value of S_v , then the test sample belongs to Class D. As can be seen, the fuzzy integral get the "non-linear" mean-value of $h(x)$. Since fuzzy measurements are from the classification accuracy of different categories, taking it as references when calculate the mean-value of multi-classification can reduce the uncertainty of multi-classifier.

Table 5: results of fuzzy measure and fuzzy integral

Defect Type	$h(x)$	$g(\bullet)$	S_v
A spike	[0.5423 0.3525 0.2514]	[0.3411 0.6878 1.0000]	0.3525
B particulate	[0.2352 0.2024 0.1375]	[0.3263 0.6121 1.0000]	0.2352
C suspended	[0.4686 0.4515 0.1554]	[0.3396 0.6794 1.0000]	0.4515
D air	[0.7445 0.6673 0.5186]	[0.3419 0.6530 1.0000]	0.6673

Take DP as blurred density, to make fuzzy integral decision for various types of partial discharge samples, it can be seen that the recognition accuracy of error-prone categories' sample (such as C, D) has significantly improved with fuzzy integral fusion decision. Because differences among original characteristic vectors of error-prone sub-sample is small, the randomness and uncertainty of recognition process make it difficult to correctly classify. Multiple classifier fusion analysis based on fuzzy integral can avoid this kind of "uncertainty" and improve the recognition accuracy to some extent.

Table 6: Classification results of Fuzzy Integral Fusion

defect model	Total number of testing samples	total number of training samples	accuracy
A spike	1000	500	94%
B particulate	1000	500	95%
C suspended	1000	500	89%
D air	1000	500	91%

In many classification problems, they are not independent of each other but there is interaction between the various classifiers. The non-additive fuzzy measurements can describe interactions between classifiers and fuzzy integral based on fuzzy measurements has become a new tool of multi-classifier fusion process. Taking the interaction between classifiers into consideration can improve the classification accuracy and enhance the fault tolerance of the fusion system. A comparison chart of this method's diagnostic accuracy is shown in figure 5.

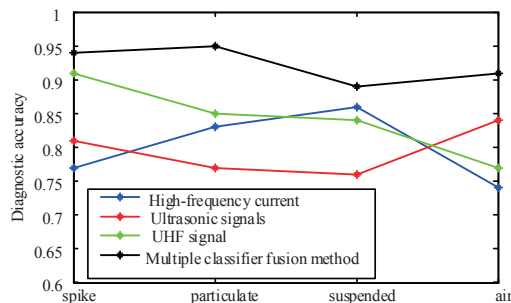


Figure 5: comparison chart of diagnostic accuracy



Figure 6: Test interval physical map

4. Field application examples of combined diagnosis of partial discharge based on the multi-dimensional characteristic parameters

One day in 2016 (ambient temperature: 36°C, relative humidity: 48%), the GIS of a 500kV substation was detected by the multi parameter local discharge analysis and diagnosis system. UHF PD signals were detected at the 500kV GIS, 2016, 4,, including the built-in sensors, grounding switch insulators and live display devices. The ultrasonic signal was detected at the connecting tube under the casing of 500kV GIS, and the defect was preliminarily located in the gas chamber of the knife. The equipment in physical diagram is shown in Figure 6.

The site detection position is shown in Figure 7. The graph (a) is a 5062C phase circuit breaker with a built-in sensor, and the diagram (b) is the insulation of the gas chamber of the 5062C-2 knife.



Figure 7: 5062C phase circuit breakers built in sensor

The PRPS diagram and the PRPD diagram are shown in Figure 8. The background map of the detection location is shown in Figure 9. As we can see from Figure 8, the signal has obvious phase characteristics, the amplitude is basically equal and has exceeded the detection range.

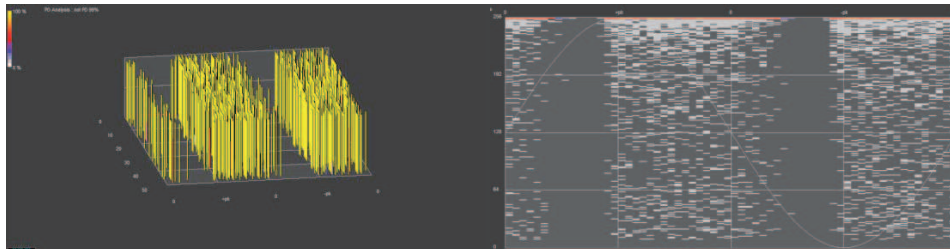


Figure 8: 5062C phase circuit breaker's built-in sensor PRPS diagram and PRPD diagram

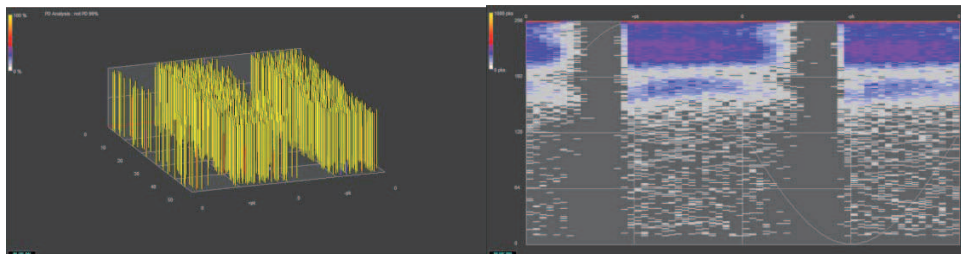


Figure 9: PRPS diagram and PRPD diagram at the insulation parts of the 5062C-2 knife sluice gas chamber.

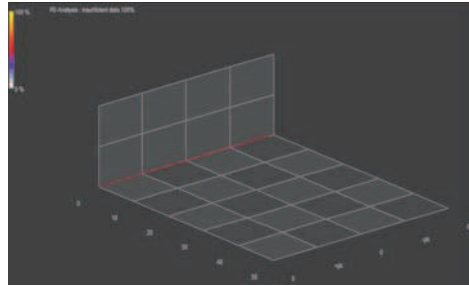


Figure 10: Background map of gas chamber insulation of 5062C-2 knife gate

The maximum amplitude of the signal is measured when the UHF sensor is placed in the insulating part of the charged display device of the 5062C-2 knife gas chamber. The test location is shown in Figure 11.



Figure 11: Insulation of the live display device of the 5062C-2 Knife Gate gas chamber

The PRPS and PRPD diagram, as shown in Figure 12, are analyzed, and the signal is a suspension potential discharge.

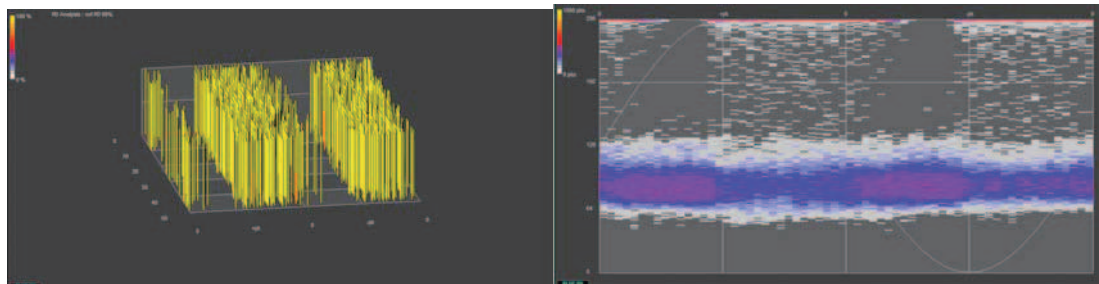


Figure 12: PRPS diagram and PRPD diagram at the insulation parts of the live display device of the 5062C-2 Knife Gate gas chamber

In June 22nd, the 5062C phase circuit breaker gas chamber was retested. The test results were in

accordance with the 20 day, and the PRPS diagram was shown as pattern 13.

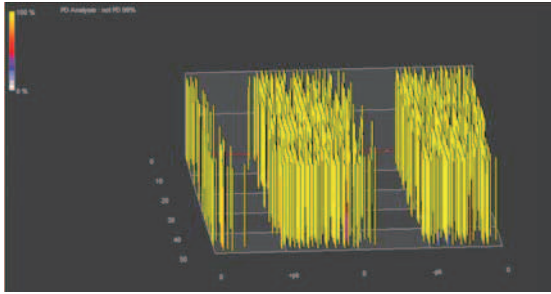


Figure 13: PRPS diagram of built-in sensor for 5062C phase circuit breaker



Figure 14: Layout of UHF sensor

The location of the defects is 1, 2 and 3. They are the built-in sensors, the grounding switch insulators and the live display devices. The location is shown in Figure 14.

The positioning results are shown in Figure 15, in which (a) a time difference mapping of the measurement point 3 and the test point 2, and (b) a time difference location map of the test point 2 and the test point 1. The measuring point 3 sensors take the lead in measuring the discharge signal. The time difference between point 3 and point 2 is 6.95ns, and the equivalent distance is approximately 2.1m. The time difference between point 2 and point 1 is 14.45ns, and the equivalent distance is approximately 4.3m, which is the same as the actual interval between point 2 and 1.

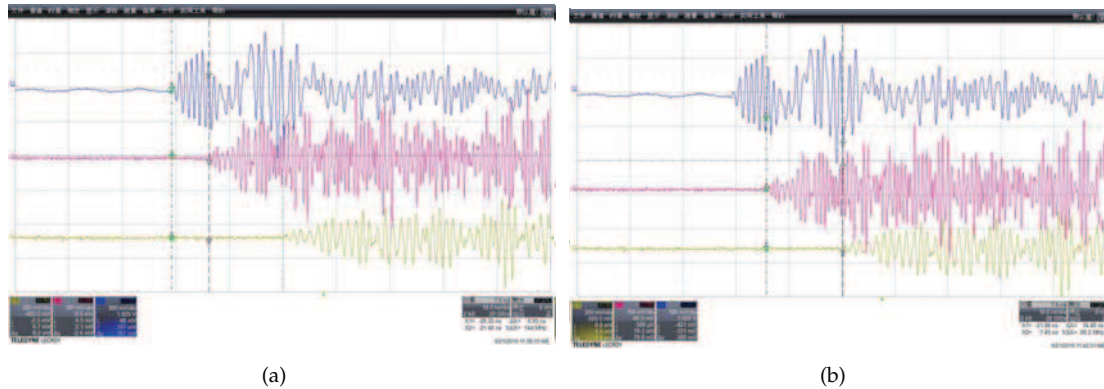


Figure 15: Point map of time difference

The measured distance of the three measuring points is shown in Figure 16, the equivalent distance between measuring point 1 and measuring point 2 is consistent with the measured distance, the equivalent distance between point 3 and point 2 is 2.1m, and the actual measuring distance is 2.3m. Point 3 detected a discharge signal earlier than point 2. The comprehensive analysis shows that the defects are located in the vicinity of the live display device and the insulated pot at the root of the casing, that is, near the measuring point 3.

5. Conclusion

This article proposes nine PD basic characteristic parameters to reflect insulation of device and 8 phase characteristic parameters to reflect the type of discharge. The collected signals are processed with the method of high frequency, UHF and ultrasonic. With the multi-classifier fusion method based on multi-parameter fuzzy integral, integrate all kinds of defects fault probability matrix, namely the diagnosis results

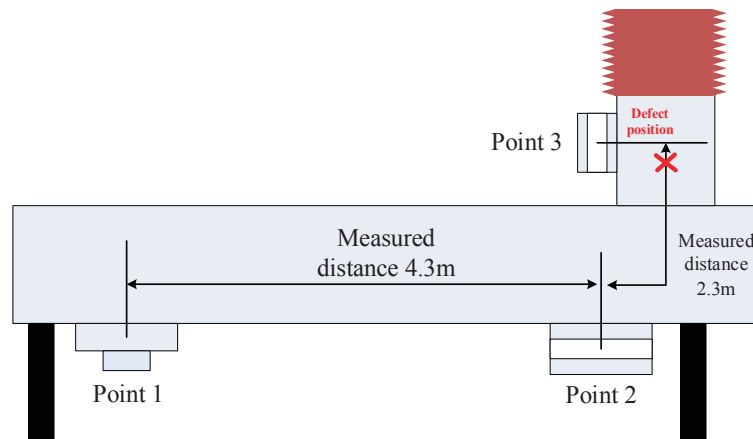


Figure 16: Discharge defect positioning diagram

of high-frequency current PD data's diagnostic method based on information fusion and semi-supervised learning ultrasonic signals diagnostic method based on adaptive mutation parameters of particle entropy and UHF signal diagnostic method based on neural network IIA-ART2A. Then calculate the final diagnosis. The diagnostic results show that this method is significantly better than single detection method when diagnose defects of spike, particulate, suspended and air.

References

- [1] Dong-suk Kim, Chul-min Hwang, Young-noh Kim, et al. Development of an intelligent spacer built into the internal-type UHF partial discharge sensor[C]. ISEI 2008. Conference Record of the 2008 IEEE International Symposium on Electrical Insulation, Vancouver, BC, Canada, 2008, pp.396-399.
- [2] S. Kaneko et al. Detecting characteristics of various type antennas on partial discharge electromagnetic wave radiating through insulating spacer[J]. IEEE Transactions on Dielectrics and Electrical Insulation, 2009, Vol. 16, No. 5, pp.1462-1472.
- [3] R.Schwarz, M.Muhr, S.Pack. Partial discharge detection in oil with optical methods[J]. IEEE International Conference on Dielectric Liquids, 2005.
- [4] Sahoo et. al: Trends in partial discharge pattern classification: a survey[J]. IEEE Transactions on Dielectrics and Electrical Insulation Vol. 12, No. 2; April 2005: 246-262
- [5] Wensheng Gao, Dengwei Ding, and Weidong Liu. Research on the typical partial discharge using the UHF detection method for GIS. IEEE transaction on power delivery, 26(??)(2011) 2621-2629.
- [6] Tapan K Saha. Review of modern diagnostic techniques for assessing insulation condition in aged transformers[J]. IEEE Transactions on Dielectrics and Electrical Insulation. 2003. 10(5): 903-917.
- [7] John A. Rice. Mathematical statistics and data analysis [M]. Thomson, 2007.
- [8] Alexander I. Galushkin. Neural Networks Theory[M]. Springer -Verlag Berlin Heidelberg, 2007.
- [9] Jian Li, Caixin Sun, Ji Yang. Adaptive denoising for PD online monitoring based on wavelet transform[C]. Proceedings of the IEEE Southeast Conference, 2006: 71-74.
- [10] X.Ma, C.Zhou, I.J.Kemp. Interpretation of wavelet analysis and its application in partial discharge detection[J]. IEEE Trans. Dielect. Elect. Insul., 2002, 9 (??): 446-457.
- [11] X.Zhou, C.Zhou, I.J.Kemp. An improved methodology for application of wavelet transform to partial discharge measurement denoising[J]. IEEE Transactions on Dielectric and Electrical Insulation, 2005, 12(??): 586-594.
- [12] Sorenson H W . Least-squares estimation: from Gauss to Kalman[J]. IEEE Spectrum, 1970, 7(7): 63-68.
- [13] Wu K, Shen W , Meng Y P, et al. The optimization of multi-parameter insulation diagnosis[C]. 2009 Annual Report Conference on Electrical Insulation and Dielectric Phenomena. Harbin, China: [s. n], 2009: 73-76.
- [14] Wu K, Shen W , Meng Y P, et al. The reliability of multi-parameter insulation diagnosis[J]. IEEE Transactions on Dielectrics and Electrical Insulation, 2010, 17(??): 280—286.
- [15] Gulski E, Kreuger F H. Computer-aided recognition of discharge sources[J]. IEEE Transactions on Electrical Insulation, 2002, 27(??): 82-92.
- [16] Montanari G C. Aging and life models for insulation system based on PD detection[J]. IEEE Transactions on Dielectrics and Insulation, 1995, 2(??): 667-675.
- [17] Lixing Zhou, Weiguo Li. Application of chaotic oscillator to partial discharge signal detection[C]. Proceedings of IEEE ICICS 2005, Bangkok, Thailand, 752-756.